*Biology of Reproduction*, 2018, 98(4), 593–606
doi:10.1093/biolre/ioy009
Research Article
Advance Access Publication Date: 17 January 2018



Research Article

# Heat exposure induces oxidative stress and DNA damage in the male germ line†

**Brendan J. Houston*, Brett Nixon, Jacinta H. Martin, Geoffry N. De Iuliis, Natalie A. Trigg, Elizabeth G. Bromfield, Kristen E. McEwan and R. John Aitken**

Priority Research Centre for Reproductive Science, School of Environmental and Life Sciences, Discipline of Biological Sciences, University of Newcastle, Callaghan, New South Wales, Australia

***Correspondence**: School of Environmental and Life Sciences, Discipline of Biological Sciences, University of Newcastle, Callaghan, NSW 2308, Australia. Tel: +61 24921 2043; Fax: +61 24921 6308; E-mail: brendan.houston@uon.edu.au

†**Grant support:** BJH was the recipient of an Australian Postgraduate Award PhD scholarship.
Edited by Dr. Monika A. Ward, PhD, University of Hawaii John A. Burns School of Medicine

Received 13 August 2017; Revised 19 December 2017; Accepted 15 January 2018

## Abstract

The reproductive consequences of global warming are not currently understood. In order to address this issue, we have examined the reproductive consequences of exposing male mice to a mild heat stress. For this purpose, adult male mice were exposed to an elevated ambient temperature of 35°C under two exposure models. The first involved acute exposure for 24 h, followed by recovery periods between 1 day and 6 weeks. The alternative heating regimen involved a daily exposure of 8 h for periods of 1 or 2 weeks. In our acute model, we identified elevated sperm mitochondrial ROS generation ($P < 0.05$), increased sperm membrane fluidity ($P < 0.05$), DNA damage in the form of single-strand breaks ($P < 0.001$), and oxidative DNA damage ($P < 0.05$), characteristic of an oxidative stress cascade. This DNA damage was detected in pachytene spermatocytes ($P < 0.001$) and round spermatids ($P < 0.001$) isolated from testes after 1 day heat recovery. Despite these lesions, the spermatozoa of heat-treated mice exhibited no differences in their ability to achieve hallmarks of capacitation or to fertilize the oocyte and support development of embryos to the blastocyst stage (all $P > 0.05$). Collectively, our acute heat stress model supports the existence of heat susceptible stages of germ cell development, with the round spermatids being most perturbed and spermatogonial stem cells exhibiting resistance to this insult. Such findings were complemented by our chronic heat stress model, which further supported the vulnerability of the round spermatid population.

## Summary Sentence

Environmental heating induces a state of oxidative stress in the male germ line, affecting multiple germ cell types; primarily the round spermatid and pachytene spermatocyte populations.

**Key words:** environment, sperm, spermatogenesis, sperm DNA fragmentation.

## Introduction

It is well established that the testis and epididymis of a majority of mammalian species are adapted to operate at temperatures 2°C–7°C below core body temperature as a consequence of being accommodated within a scrotal sack [1–3]. Although the adaptive significance of the cooler environment afforded by the scrotum is still being actively debated, it has been proposed that this temperature differential maintains optimal spermatogenesis, minimizes gamete mutation rates, and/or supports sperm maturation and storage in the epididymis [4]. Accordingly, these organs and the male germ line they support are susceptible targets for heat stress arising from inguinal clothing and/or elevated ambient temperatures. Indeed, it

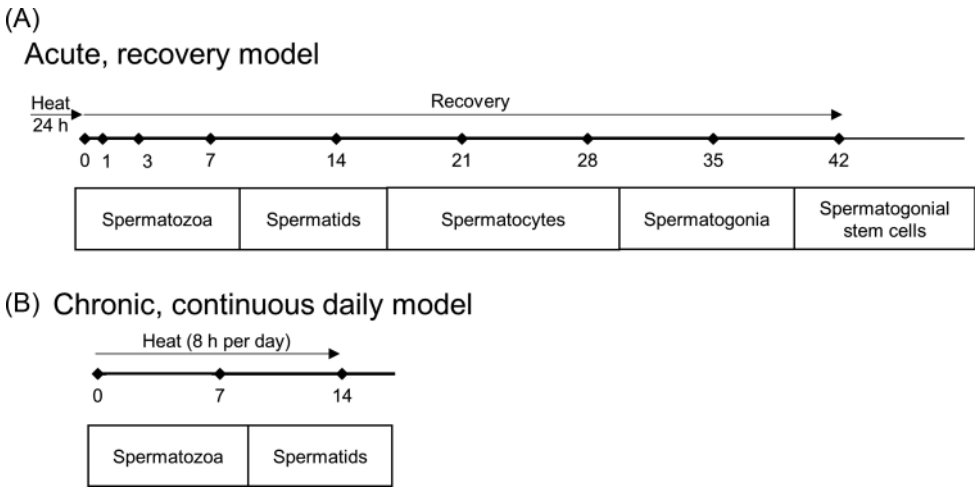


**Figure 1.** Ambient temperature heat treatment regimens. Mice were treated with heated environmental conditions at a temperature of 35°C and 30% humidity under an acute or chronic exposure approach. Each major stage of germ cell development insulted by heat treatment is documented. This corresponds with specific recovery times taken to mature to spermatozoa, whereby cells were collected in the cauda epididymidis. (A) Acute exposure model: mice were heated for 24 h continuously, and then removed from heating conditions and allowed to recover for 1 day to 6 weeks. (B) Chronic-like model: mice were heated for 8 h per day for a period of 1 or 2 weeks, then assayed the following day.

is well documented that heat stress negatively impacts male reproduction, affecting multiple stages of spermatogenesis and driving an overall reduction in sperm count, motility and normal morphology [1, 5, 6]. It follows that men who are occupationally exposed to extreme heat conditions commonly experience spermatogenic arrest, characterized by the onset of azoospermia, oligozoospermia, or teratozoospermia [7], and exhibit reduced fertility and sperm counts in summer months across the world [8–11]. This situation is compounded in our species owing to relatively low fertility arising from reduced semen quality [12, 13], a response that has been increasingly linked to a variety of adverse environmental exposures [13].

Interest in the effects of thermal stress on male fertility has spanned many decades, with the deleterious nature of this stress on testicular function first being identified in studies reported throughout the 1920s and 1940s in species such as the human, rabbit, and rat [14–16]. In seeking to account for the mechanistic basis of this damage, it has been proposed that the most heat sensitive stages of germ cell development correspond to the spermatids and the pachytene spermatocytes [5, 17–19]. Both of these germ cell populations exhibit elevated levels of DNA damage in response to acute heat stress, resulting in significant reductions in the success of embryonic development achieved following fertilization of oocytes once these cells mature to spermatozoa. Heat stress has also the ability to impair the development of spermatocytes into spermatids [18]. In marked contrast, preceding phases of germ cell development, such as type A spermatogonia, appear relatively resilient to heat stress [20]. This leads to a situation whereby the immediate postheating reduction in germ cell proliferation and sperm quality is progressively ameliorated as the unaffected type A spermatogonia mature to replenish the damaged pool of spermatids and pachytene spermatocytes [19].

Notably, while many of the preceding studies were designed to investigate the effects of localized heating on the testis, and therefore mimic conditions experienced in response to inguinal clothing, the comparative impact of ambient temperature heating models where the whole body is subjected to thermal stress remains less well studied. In those studies that have sought to address this paradigm, it has been shown that spermatozoa exhibit hallmarks of apoptosis [3, 21] and are significantly less competent at supporting embryo development [19] following exposure to an elevated temperature of 35°C for as little as 24 h. It has been identified that the production of reactive oxygen species is a common outcome of heat stress in male germ cells [1], which suggests that this insult is capable of inducing a state of oxidative stress. However, a mechanistic explanation for the embryonic losses associated with such stress has not been established. Furthermore, an extensive investigation of spermatogenesis, sperm quality, and function under conditions of ambient heat stress has not been undertaken. In this study, we sought to refine our understanding of the molecular and functional changes induced in spermatozoa in relation to the decreased fertility observed after either acute or chronic elevation of ambient temperature.

## Materials and methods

The chemicals and reagents used in this study were purchased from Sigma Aldrich (Sigma Chemical Co., St. Louis, MO, USA) unless stated otherwise, and were of research grade. The fluorescent probes were purchased from Thermo Fisher Scientific (Waltham, MA, USA), unless otherwise stated. All fluorescent imaging was performed using a Zeiss Axioplan 2 fluorescence microscope (Carl Zeiss MicroImaging GmbH, Jena, Germany).

### Heating exposure regimens

Experimental protocols were approved by the University of Newcastle Animal Care and Ethics Committee (Ethics number 2014–447). Male C57BL/6 mice were exposed to heated environmental temperature in an animal intensive care unit cage (Lyon Technologies, Chula Vista, CA, USA). These mice were at least 8 weeks of age, with food and water provided ad libitum. Exposure (see Figure 1) was performed for either 24 h at 35°C and 30% humidity (acute heat stress) or for 8 h per day under the same conditions for 1 or 2 weeks (chronic heat stress). Following exposure, the 24 h treated mice were allowed to recover over a period of 1 day to 6 weeks and were then culled. This timing of recovery was selected to correspond to the maturation of each major stage of germ cell development through to spermatozoa (see Figure 1A). For the chronic 8 h per day exposures,

the mice were culled the following day after the final heat treatment to gain insight into the effect of multiple heating treatments on sperm quality (see Figure 1B). This approach was designed to provide insight into these effects on the spermatozoa in the epididymis and also the spermatids, which were believed to be particularly heat vulnerable. Spermatozoa were collected from the cauda epididymidis and assayed for impacts of heating on cell activity and function as described below. Five mice were utilized for each time point, unless otherwise stated.

## Isolation of reproductive organs and spermatozoa

### Dissection

Epididymides and testes were dissected from adult C57BL/6 mice immediately after being culled via $CO_2$ asphyxiation. Where required, mature spermatozoa were isolated from the cauda epididymidis by retrograde perfusion via the vas deferens [22]. One testis and one epididymis (fitted to a plastic grid) were placed in a Bouin fixative (9% formaldehyde, 5% acetic acid, 0.9% picric acid) for 6 h at 4°C in a rotator. These tissues were then resuspended in 70% ethanol overnight at 4°C in a rotator. Finally, the residual Bouin fixative was washed out through resuspension in 70% ethanol and the tissues were stored at 4°C in preparation for sectioning. One section from each testis and epididymis was stained with hematoxylin and eosin to investigate testis and epididymal morphology. Three sections per treatment were assessed for morphological abnormalities in comparison to control tissue. Here, the presence of maturing germ cells and spermatozoa in the seminiferous tubules of the testis was evaluated. The presence of spermatozoa and morphologically normal tubules across the three principal regions of the epididymis was also evaluated.

### Collection of spermatozoa and assessment of motility and vitality

Spermatozoa were isolated from the cauda epididymidis into microcapillary tubes by a method of retrograde perfusion and further released into BWW medium [22, 23]. Objective sperm motility was then assessed by computer-assisted sperm analysis (CASA; IVOS, Hamilton Thorne, Danvers, MA, USA) as previously detailed [22], with a minimum of 100 spermatozoa in the five fields analyzed. The following settings were modified: minimum cell size of 9 pixels, minimum contrast of 80, low size gate of 0.3, high size gate of 1.95, low intensity gate of 0.5, high intensity gate of 1.3, nonmotile head size of 45 pixels, nonmotile head intensity of 75, average path velocity (VAP) threshold of 10 $\mu$m/s, and threshold straightness (STR) of 75%. Cells exhibiting a VAP of 10 $\mu$m/s and an STR > 0 were considered progressive. Cells with a VAP greater than that of the mean VAP of progressive cells were considered rapid. Sperm vitality was assessed via the eosin exclusion method ([24]) using a dilution of 1:1.

### Germ cell isolation

Enriched pachytene spermatocyte and round spermatid populations were isolated from 1 day acute heat-treated testes as previously described [25]. Routine assessment of germ cell purity using a DAPI nuclear stain revealed an 81% purity for pachytene spermatocytes and a 89% for round spermatids. This assessment identified the remaining cells of the pachytene spermatocyte population to be spermatocytes at the leptotene, zygotene, or diplotene stage, and in the case of the round spermatid isolation, this was represented by elongating spermatids. We did not observe the presence of peritubular myoid cells in our preparations.

## Determination of oxidative stress in spermatozoa

### Flow cytometry

Spermatozoa were assessed for oxidative stress levels via flow cytometry using the mitochondrial superoxide probe MitoSOX red (MSR) and the membrane fluidity marker Merocyanine 540 (M540) in conjunction with the Sytox Green (SYG) vitality stain. Cells were resuspended in either 2 $\mu$M MSR or 2.7 $\mu$M M540, in combination with 20 nM SYG in BWW for 15 min in the dark at 37°C. These cells were then centrifuged at 450 × g for 5 min and then resuspended in 400 $\mu$L BWW. Each sample was transferred to a flow cytometry tube for analysis with a FACS-Canto flow cytometer (BD Biosciences, San Jose, CA, USA) equipped with a 488-nm argon laser and a 633 nm helium-neon laser. Analysis of these data was undertaken using CellQuest software (BD Biosciences, San Jose, CA, USA).

### Oxidative DNA damage (8-OH-dG) immunofluorescence

Spermatozoa were snap-frozen in liquid nitrogen and stored at –80°C for the purpose of the 8-OH-dG assay. These cells were then resuspended in primary DNA/RNA damage antibody (Novus Biologicals, Littleton, CO, USA) (25 $\mu$g/ml in PBST) overnight at 4°C. Following incubation, spermatozoa were washed in PBS and then incubated with AlexaFluor 488 goat $\alpha$ mouse secondary (5 $\mu$g/ml in PBS) for 1 h at 37°C, washed twice in PBS, and placed on slides for viewing with fluorescence microscopy. A sample of 100 cells was assessed for this analysis, scored positive by the presence of nuclear fluorescence.

## Immunohistochemistry

Paraffin-embedded tissue sections were dewaxed and utilized for antigen retrieval by microwaving in a solution of 50 mM Tris (pH 10.5) for 9 min. Each section was blocked in 3% bovine serum albumin (BSA)-PBST for 1 h at room temperature and washed in PBS for 5 min. Following this, primary antibody incubation was performed with DNA/RNA damage antibody (8-OH-dG; Novus, Littleton, CO, USA) or cleaved caspase-3 (Abcam 13487) (both at 5 $\mu$g/ml) overnight at 4°C. For tubulin, a conjugated primary antibody was used (2.5 $\mu$g/ml) for 1 h at 37°C. Slides were then washed three times in PBS for 5 min. Secondary antibody incubation was undertaken in 1% BSA-PBST for DNA/RNA damage using AlexaFluor-594 (Thermo Fisher Scientific) conjugated $\alpha$-rabbit or $\alpha$-goat antibodies (10 $\mu$g/ml) for 1 h at 37°C. Slides were washed three times in PBS for 5 min and counterstained with DAPI (0.5 $\mu$g/ml) for 5 min at room temperature and mounted in Mowiol 4–88 (Millipore, Darmstadt, Germany) prior to viewing under a Zeiss Axioplan 2 fluorescence microscope (Carl Zeiss MicroImaging GmbH, Jena, Germany). For 8-OH-dG quantification, a minimum of 15 seminiferous tubules or cauda epididymal tubules were utilized for mean pixel intensity assessment through ImageJ software (NIH, USA). This quantification was restricted to only the germ cells within the seminiferous tubules of the testis, or only the lumen of the cauda tubules containing the sperm population. Three replicates were performed for each treatment.

### TUNEL (Apop-Tag kit, Millipore)

Tissues sections were dewaxed and rehydrated as detailed above, and this procedure was carried out as per the manufacturer's protocols.

Antigen retrieval was then performed with 20 $\mu$g/ml proteinase-K/PBS for 10 min at room temperature, and DNase enzyme (Roche) was used for the positive control. Following preparation, slides were washed thrice in PBS and mounted in Mowiol 4–88 with antifade for viewing with fluorescence microscopy. This analysis was performed using mean pixel intensity within seminiferous tubules through ImageJ software (NIH), excluding interstitial tissue and focusing on the germ cell population. Three replicates were performed for each treatment, and at least 10 tubules were analyzed for each slide.

### Alkaline comet assay

The comet assay was performed as described previously [26] on spermatozoa and germ cells. Diverging from this protocol, electrophoresis was performed at 1 V/cm for 3 min for spermatozoa or 4 min for precursor germ cells. SYBR green nucleic acid stain (Thermo Fisher Scientific) was applied to the slides immediately before viewing on the microscope, and a coverslip was added. The level of DNA damage was analyzed using Comet Assay IV software (Perceptive Instruments, Suffolk, UK). A collection of at least four replicates was used for each analysis, where a minimum of 30 comets were assessed and subsequently utilized for statistical analysis. For the positive control, spermatozoa were resuspended in 500 $\mu$M hydrogen peroxide for 5 min at room temperature. These cells were then washed in PBS, and then resuspended in PBS.

### Sperm capacitation, oocyte binding, and fertilization assays

Mature oocytes were retrieved from the distal ampullae of 3- 4-week-old C57BL/6 female mice following superovulation as previously described [27]. Spermatozoa were simultaneously capacitated and then co-incubated with oocytes for 4 h at 37°C [27], after which signs of successful fertilization (extrusion of the second polar body and/or pronucleus formation) were analyzed blindly. The percentage of fertilized oocytes and percentage of embryos that had reached the blastocyst stage by the morning of day 5 were calculated.

### Immunofluorescence of spermatozoa

Spermatozoa were fixed in 4% paraformaldehyde for 15 min at room temperature, washed twice in 0.05 M glycine, and then stored in this solution at 4°C for peanut agglutinin (PNA) or phosphotyrosine (pt66) staining. A sample of $2 \times 10^6$ cells was then treated with 0.1% Triton-X100 in PBS for 10 min at room temperature, followed by washing in PBS. These cells were then labeled with primary antibody (4 $\mu$g/ml pt66) or conjugated PNA lectin (2.5 $\mu$g/ml) in PBS for 1 h at 37°C. The cells were washed once in PBS, and pt66 samples were then treated with AlexaFluor 488 goat $\alpha$ mouse secondary antibody (5 $\mu$g/ml in PBS) for 1 h at 37°C. After a final wash in PBS, cells were placed on slides and viewed via fluorescence microscopy.

### Statistical analysis

JMP version 11 (SAS Institute Inc., Cary, NC) was used to analyze the data in each experiment, which were performed with at least five independent replicates (unless stated otherwise). Normality of these datasets was assessed with the Shapiro-Wilk test ($\alpha = 0.05$). Following this, a one-way ANOVA was used to compare normally distributed treatments with a post hoc Tukey honest significant difference test ($\alpha = 0.05$). For data that were not normally distributed, or where the number of replicates was limited to 3, the Wilcoxon test was used ($\alpha = 0.05$), with a post hoc Dunn test. Error bars represent mean values ± standard error of the mean.

## Results

In order to confirm the stability of the ambient temperature environment generated by the heating apparatus employed in these studies, we first assessed the ambient temperature within the device over a 24-h time course using a sensitive temperature probe (Figure 2A). Here, we observed a very consistent heating output of 35°C, with only small fluctuations of +0.5°C at few instances during this time course. Presented with a reliable heating treatment, we proceeded with our experimental exposure regimen. During the initial, acute exposure treatment, we documented the weight of all mice during their recovery period of up to 6 weeks, revealing no significant changes in weight associated with heat stress (Figure 2B). Furthermore, investigation of the testis: body weight ratios across all treatment methods confirmed no gross fluctuations (Figure 2C). When investigating the ability of the mice to manage the temperature insult (Supplementary Figure S1), it was apparent that this treatment did not alter body temperature, which was measured at the arm pit, the testis, and the back. Here, the mice were capable of regulating their body at temperature under an ambient heat of 35°C.

### The effects of heating on spermatogenesis and testis structure

Next, we probed the effect of acute heating on spermatogenesis via an initial examination of the gross morphology of the testis (Supplementary Figure S2). Testes from mice subjected to recovery periods of either 1 day, 2 weeks, or 6 weeks (encompassing the beginning, middle, and end of our recovery periods) were assessed, revealing no dramatic changes in any of the treatment groups. Indeed, each testis section was characterized by equivalent morphology (Supplementary Figure S2A) and encompassed all stages of germ cell maturation including the presence of spermatozoa in the center of the seminiferous tubules. To complement this analysis of the morphology of the germ cells postheating, we explored the expression of $\alpha$-tubulin in the testes of these mice (Supplementary Figure S2B). As anticipated, tubulin was expressed widely throughout the seminiferous tubules, with predominant labeling detected at the periphery of the early stage germ cells, within the developing acrosomal vesicle and within the flagellum of spermatozoa. In this regard, we did not observe any apparent modifications to the expression of this protein, or the structural elements in which it resides, across any of the treatments.

To extend these data, we next investigated whether acute heating was capable of inducing DNA damage to germ cells and spermatozoa residing in the testis of exposed males. First, the testis sections were probed for single-strand DNA breakage using an Apop-Tag TUNEL kit (Figure 3). This analysis revealed a significant increase in TUNEL-positive germ cells in the testis of heat-treated animals that were allowed 1 day recovery post-treatment ($P < 0.001$), in a similar fashion to that of our positive control ($P < 0.001$). Notably, by 2 and 6 weeks postheat stress, the bulk of TUNEL-positive cells had apparently been resolved such that the intensity of this labeling was indistinguishable from that of untreated controls. The DNA damage detected in this fashion was, however, not imminent of an apoptotic death, as highlighted by the lack of overt cleaved caspase-3 expression in the testicular germ cells in response to heat exposure (Supplementary Figure S4). Furthermore, heat exposure did not induce elevated DNA double-strand break formation in any cell type (bar a typical level demonstrated in early meiotic cells) as detected via phospho gamma-H2AX staining (data not shown). Finally, to investigate the induction of

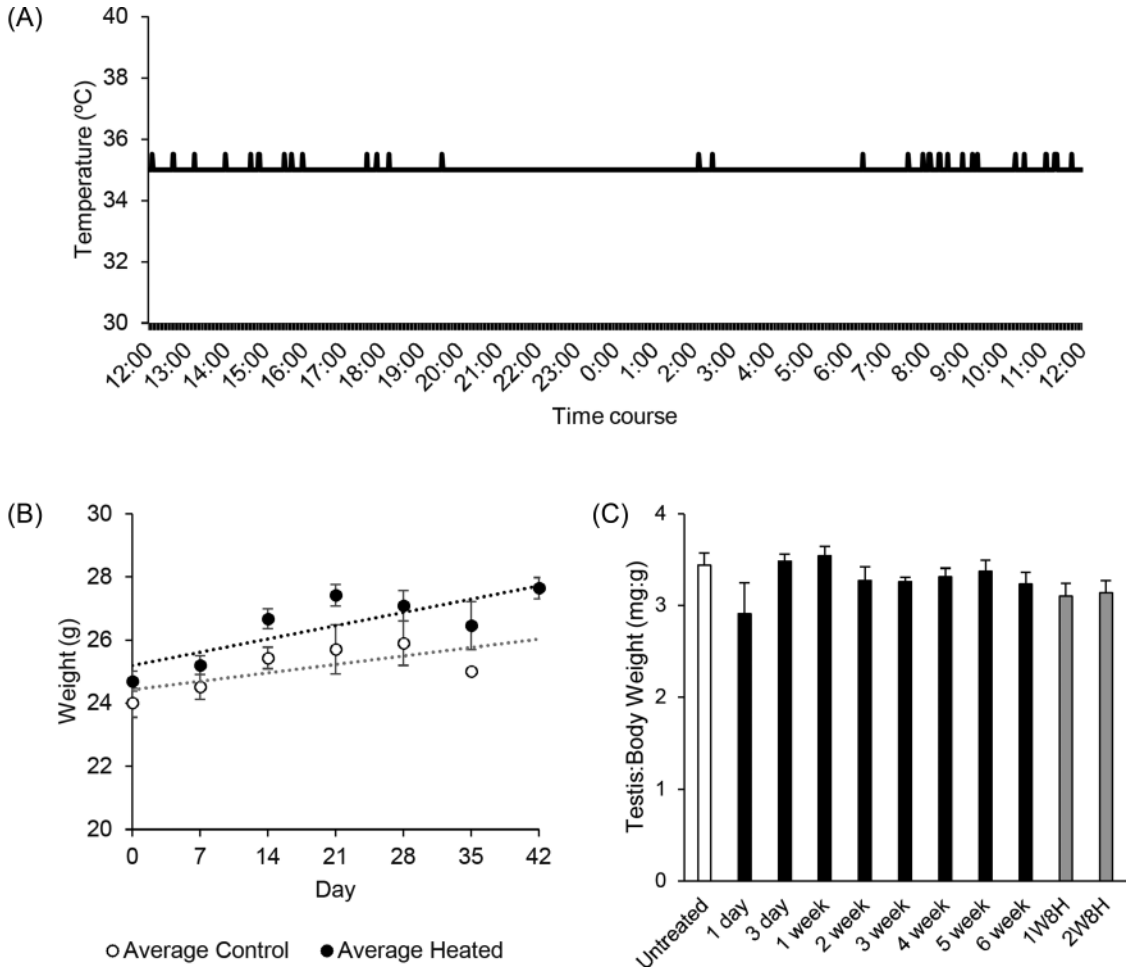


**Figure 2.** Heating machine stability and growth of mice with heat treatment. (A) Temperature reading of heating apparatus over a 24-h period. (B) Mice were weighed weekly to determine growth of untreated and acute heat-treated populations over the 6-week recovery period. (C) Testis: body weight of mice from all treatment groups.

oxidative stress in response to heat stress, testis sections were probed with an antibody capable of detecting 8-hydroxy-2'-deoxyguanosine (8-OH-dG), a mutagenic base byproduct arising from oxidative DNA damage (Figure 4). This marker peaked in expression 2 weeks postheating to a significant degree ($P = 0.05$), and subsequently returned to basal, untreated, levels with a period of 6 weeks of recovery.

## The effects of heating on the epididymal structure and epididymal sperm maturation

To complement the analysis of testicular response to heat stress, we undertook a similar evaluation of the impact of heating on the epididymis (Supplementary Figure S3), an organ with a pivotal role in regulating the post-testicular maturation of spermatozoa. Consistent with the testes, we observed no overt abnormalities in the gross epididymal morphology following exposure of males to acute heat stress. Indeed, at each recovery timepoint examined, epididymal sections exhibited similar epithelial cell morphology and the lumen of all epididymal sections was replete with spermatozoa. Finally, to investigate oxidative DNA damage levels of the spermatozoa in the epididymis, these sections were incubated with an anti-8-OH-dG antibody and again assessed via mean pixel intensity with respect to caudal spermatozoa (Figure 5). Here, the levels of spermatozoa bearing signatures of oxidatively damaged DNA remained constant in all stages of heat exposure (1 day, 2 weeks, and 6 weeks of recovery).

## Heating induced declines in sperm quality

In contrast to the minimal effects of acute heat stress on the overall structure of the testis and epididymis, such treatment induced an immediate, highly significant impairment of overall and progressive motility ($P < 0.001$) (Figure 6A and B). The negative impact on these parameters was evident at 1 and 3 days post-treatment in our acute heat-exposure model. However, this apparent reduction in overall and progressive sperm motility was ameliorated over time, with as little as 1-week recovery resulting in a return of both motility parameters to a level that was not significantly different from the spermatozoa of untreated animals (Figure 6A and B). Furthermore, at 2 weeks postheating, corresponding to the time at which heat exposed round spermatids would be expected to occupy the cauda epididymidis, the overall levels of sperm motility were again observed to significantly decline ($P < 0.05$) (Figure 6A). Thereafter (i.e. 3–6 weeks postheating), all sperm motility parameters consistently attained a comparable level to that of the untreated controls.

To confirm these findings and additionally understand the effect of extended heating on sperm motility, we employed our chronic

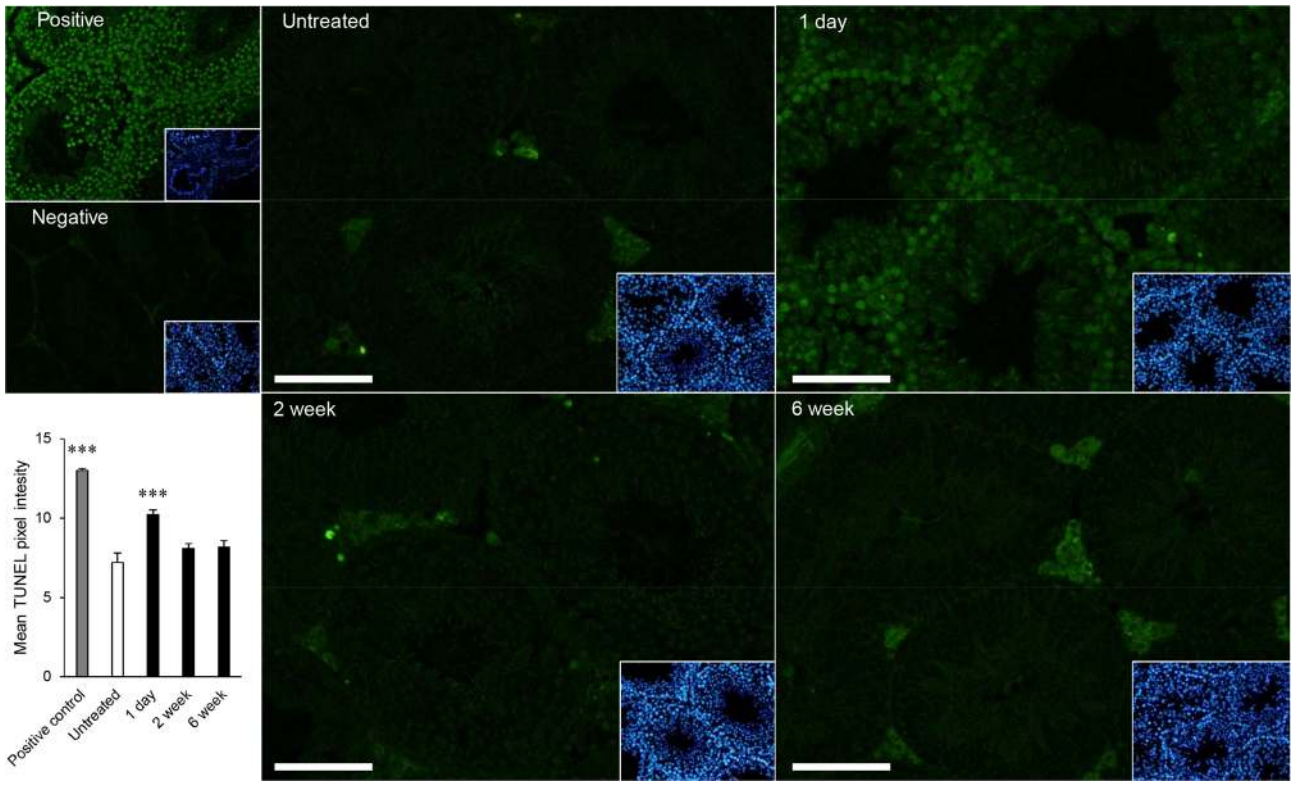


**Figure 3.** Whole body heating induced testis TUNEL staining as a marker of DNA damage. Mouse testes from 1-day, 2-week, and 6-week heat recovery treatments were fixed and sectioned for staining with an ApopTag TUNEL kit. Pixel intensity was used to quantify staining, which is displayed as a graph alongside the images. DNase was used as the positive control. *** $P < 0.001$ compared to untreated control. Staining was performed on three independent replicates (n = 3). Scale bar = 200 $\mu$m.

heating model of 8 h per day for 1–2 weeks (gray bars). This chronic exposure model was used to investigate the effects of continuous heat exposure on the epididymal spermatozoa (1-week recovery) and particularly the maturing spermatids (2-week recovery), as we detected a potential susceptibility of the latter cell population to heat stress in our acute model above. The chronic heating regimen was also associated with a significant reduction of sperm motility ($P < 0.05$), with both exposure periods (1 and 2 weeks) generating similar results (both 49% vs 70% in untreated controls). When comparing progressive sperm motility (Figure 6B), we again observed a similar decline across both exposure lengths. This was comparable to our acute model, where both 1 and 3 days postacute heating (black bars) and 1 and 2 weeks of daily heating (gray bars) elicited significant declines in this key motility parameter ($P < 0.001$; $P < 0.05$, respectively). However, when the velocity of the spermatozoa was analyzed it was found that their average path velocity (VAP; Figure 6C), straight line velocity (VSL; Figure 6D), and linearity (LIN; Figure 6E) were all significantly compromised in the chronic exposure model ($P < 0.01$) but not acute, recovery treatment regimes. One final measure of sperm motility, amplitude of lateral head displacement (ALH; Figure 6E), remained constant across all treatment types.

## The involvement of oxidative stress in the heat stress response of spermatozoa

To ascertain the involvement of oxidative stress in accounting for the heat-associated decrease in sperm quality, we next investigated the effect of heating on ROS production, lipid membrane structure, and oxidative DNA damage (Figure 7). With respect to the number of vital cells collected from heated males (Figure 7A), we observed a heat induced decline, similar to that demonstrated in our sperm motility data (Figure 6A) for our acute, recovery model. A significant decline was observed for this parameter at 1 day ($P < 0.001$), 3 days ($P < 0.01$), and 2 weeks ($P < 0.05$) postheating, but no such decline was associated with the chronic regimen in which mice were heated daily for 1–2 weeks. Investigation of mitochondrial ROS using the MitoSOX red probe (Figure 7B) identified a substantive 1.5-fold increase in oxidant generation ($P < 0.05$) 3 days postacute heating. Next we investigated sperm membrane fluidity using merocyanine 540 (M540; Figure 7C) to potentially explain the profile of heat induced modifications to motility. While a majority of the heat treatments induced a similar response to our untreated control, 2 weeks recovery from the acute heat insult again generated spermatozoa with a pronounced increase in M540 staining ($P < 0.05$), achieving a similar level of staining to that of our positive control ($P < 0.01$). As a final marker of oxidative stress, we assessed the number of spermatozoa presenting with 8-OH-dG staining (Figure 7D). Here, we observed a decline in the presence of this marker in spermatozoa recovered 3 days ($P < 0.05$) and 1 week ($P < 0.01$) postheating, followed by a substantive increase in the expression of 8-OH-dG following 2 weeks of recovery ($P < 0.05$).

## DNA fragmentation in heat-treated germ cells and spermatozoa

Of major importance to sperm function is the integrity of sperm DNA which is known to be vulnerable to oxidative stress. To

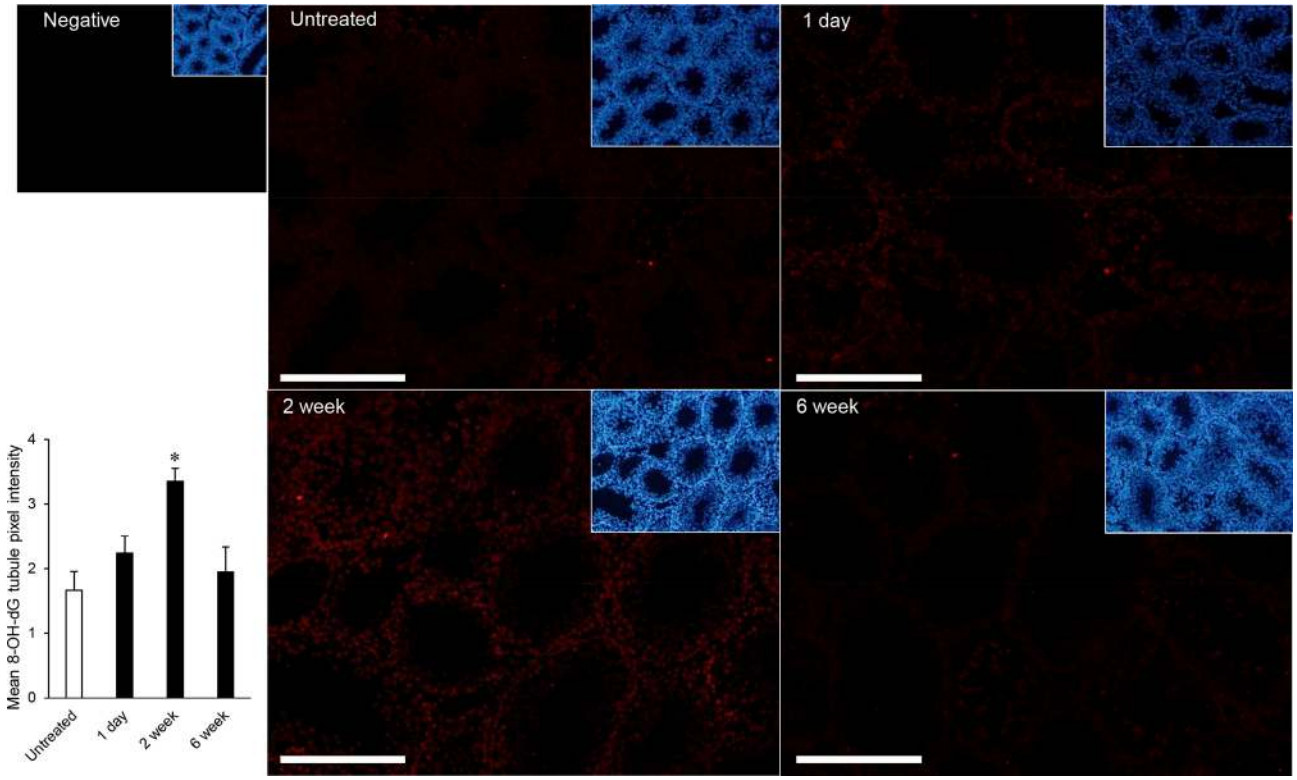


**Figure 4.** Whole body heating induced oxidative DNA damage in testicular germ cells. Mouse testes from 1-day, 2-week, and 6-week heat recovery treatments were fixed and sectioned for staining with an antibody recognizing oxidative damage. The pixel intensity of the germ cells within the tubules was quantified and is displayed alongside images. $* P < 0.05$ compared to untreated control. Staining was performed on three independent replicates (n = 3). Scale bar = 200 $\mu$m. Staining without the primary antibody was used for the negative control.

investigate the existence of such damage, we utilized the alkaline comet assay to quantify the effects of heating on the incidence of sperm DNA damage (Figure 8A). Here, we observed an immediate and significant elevation in the occurrence of DNA single-strand breaks ($P < 0.001$), 1 day postacute heat exposure. Additional vulnerable stages encompassed 2 ($P < 0.001$), 3 ($P < 0.01$), 4 ($P < 0.001$), and 5 weeks ($P < 0.001$) postacute heating recovery, and 2 weeks ($P < 0.001$), but not 1 week, of daily heat exposure. Again, both exposure models suggested that the round spermatid stage of spermatogenesis was particularly vulnerable to the induction of DNA damage, as well as proliferating spermatogonia, as proposed with 5 weeks of recovery in the acute model. To further investigate whether the appearance of such damage reflected the differential sensitivity of different stages of spermatogenesis to the effects of heat, we next isolated pachytene spermatocytes and round spermatids from 1 day acute heating recovery testes, using specialized density gradients (Figure 8B). In agreement with the sperm DNA damage data, we observed the DNA of both cell types to be particularly sensitive to heat, exhibiting significant elevations in the levels of DNA fragmentation ($P < 0.001$) when isolated from heat-treated mice. Furthermore, with respect to spermatozoa collected from the cauda epididymidis, these stages of germ cell development correspond to the 2 (round spermatids) and 3 (pachytene spermatocytes) week recovery samples in the acute setting (Figure 1).

### Fertilization capacity of acute heat-treated spermatozoa

As a final approach at determining the effects of heating on sperm function, we conducted capacitation and fertility assays, focusing on phosphotyrosine expression, acrosome integrity, zona pellucida binding capacity, and fertilization rates achieved through conventional IVF (Figure 9). Again, we utilized our 1-day, 2-week, and 6-week recovery spermatozoa to investigate the early, middle, and late periods of heat recovery in our acute model. Following stimulation of capacitation, we found no difference in the number of spermatozoa exhibiting complete tail tyrosine phosphorylation (Figure 9A) or those which had undergone a spontaneous acrosome reaction (Figure 9B). The ability of these spermatozoa to bind to the zona pellucida of salt stored oocytes (Figure 9C) was also unchanged compared to the untreated sample at all recovery time points, visually represented in Figure 9D. We next used in vitro fertilization (IVF) to ascertain how the downstream effects of impaired motility (Figure 6) and elevated DNA damage (Figures 7 and 8) impacted the functionality of the heat-exposed spermatozoa. Here, we found that all recovery groups generated spermatozoa capable of fertilizing oocytes at statistically similar rates to untreated spermatozoa (Figure 9D). This finding was also consistent with the development of these zygotes throughout early embryogenesis (Figure 9E), where we detected no significant effect of heat treatment in spermatozoa on blastocyst formation rate across all time points (1 day, 2 weeks, and 6 weeks).

## Discussion

In this study, we have demonstrated that acute and chronic exposure to elevated ambient temperature can have significant negative effects on certain aspects of sperm quality. Further, these data provide evidence to support the existence of an oxidative stress-mediated pathology in ambient heat stress. This oxidative stress manifested

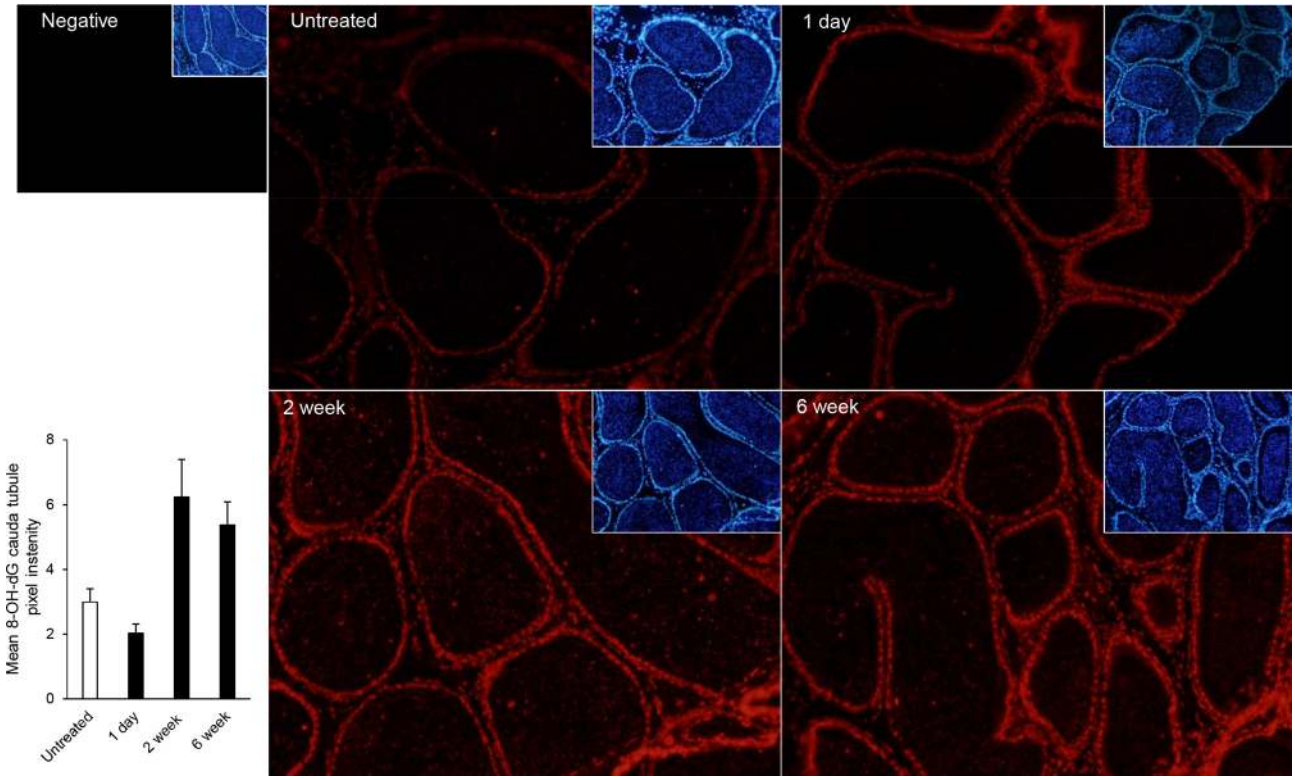


**Figure 5.** Whole body heating induced oxidative DNA damage in epididymal spermatozoa. Mouse epididymidis from 1-day, 2-week, and 6-week heat recovery treatments were fixed and sectioned for staining with an antibody recognizing oxidative damage. The pixel intensity of the spermatozoa within the lumen was quantified and is displayed alongside images. Staining was performed on three independent replicates (n = 3). Scale bar = 200 $\mu$m. Staining without the primary antibody was used for the negative control.

most significantly in spermatozoa arising from heat-stressed round spermatids, and was also clearly established in spermatozoa arising from proliferating spermatogonia, and spermatocytes, but did not adversely affect the spermatogonial stem cell population itself. With respect to sperm function, these impacts did not have overt effects on the fertilizing capacity of these spermatozoa or the resulting embryos throughout early embryonic development to the blastocyst stage.

Historically, studies investigating the effect of heating on spermatogenesis have utilized temperatures in excess of 40°C, leading to a clear impairment of the spermatogenic cycle, abnormal germ cell morphology, and loss of germ cells populating the seminiferous tubules within the testis [28–33]. In contrast, the acute heating regimen used in this study failed to elicit equivalent overt changes in the development or morphology of testicular germ cells, or in the overall structure of the testis (Supplementary Figure S2). Such findings nevertheless accord with those of Comish et al. [33], who have provided evidence that pronounced modifications of the male germline are only induced once the testis is subjected to a temperature threshold of at least 36°C. Despite this, we did detect the presence of elevated levels of oxidative DNA damage in germ cells as well as enhanced TUNEL staining in the testis of mice 1 day postheating. In agreement with previous studies [21, 31, 34], these data suggest that even relatively mild heat stress can induce DNA fragmentation within the testis. Specifically, this damage was not sufficient to elicit an apoptotic cascade as detailed by the absence of elevated cleaved caspase-3 expression (Supplementary Figure S4). This notion is further supported by the absence of disruption to spermatogenesis at any time point (Supplementary Figure S2).

In seeking to assess the ontogeny of male germ cell vulnerability to heat stress, we provided evidence that acute heat exposure elicited a negative impact on the motility parameters of those spermatozoa residing in the epididymis [35] at the time of insult. This acute heat treatment led to a rapid decline in the percentage of motile caudal spermatozoa. Additionally, when germ cells were exposed as round spermatids, the resulting populations of spermatozoa they went on to generate (i.e. at 2 weeks of recovery postheat exposure [36]) also suffered significant impairment of their overall motility ($P < 0.05$), supporting previously reported findings [5]. However, in this acute model these results are likely largely accounted for by the loss of sperm viability occurring in parallel to the declines in motility. Notably, clinical studies exploring the consequences of direct scrotal heating of the human testis, using a regimen consisting of biweekly exposure over a 3-month period, have also documented significant negative impacts on sperm motility and sperm output [6]. Similar outcomes have been described in the agriculturally important bovine model [37]. In both settings, a decline in motility during heat stress was documented, followed by a gradual recovery at the conclusion of this exposure. Thus, a common theme emerging from these studies is that, given sufficient time for recovery, the heat impairment of sperm motility is eventually repaired. Such reversibility is probably due to the enhanced resistance of the type A spermatogonia to heat stress [19], thus enabling these precursor germ cells to act as a buffering or defense mechanism to mitigate the impact of environmental threats upon spermatogenesis. This phenomenon may be explained by elevated concentrations of Cu/Zn superoxide dismutase present in spermatogonia in comparison to later stage germ cells [38], in

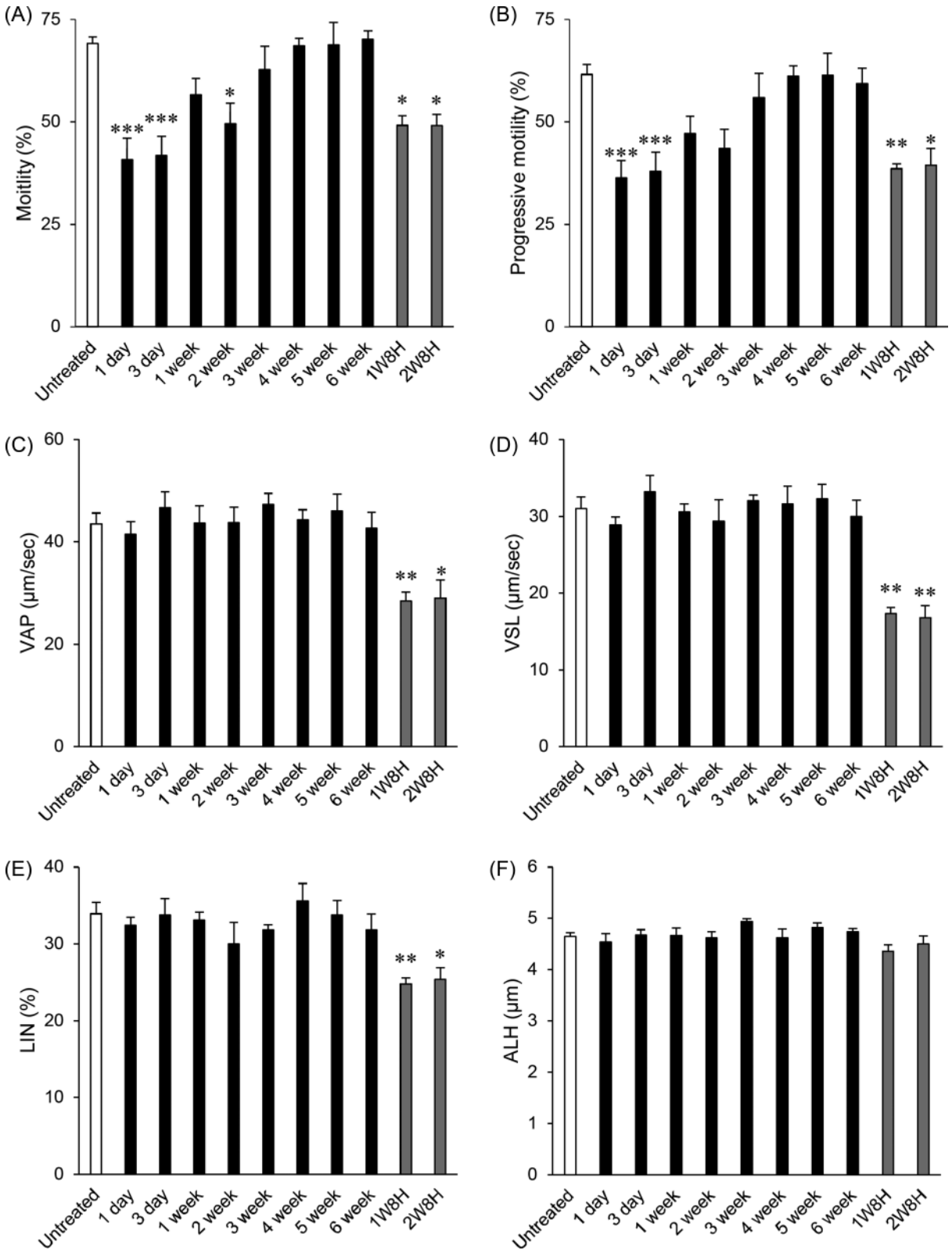


**Figure 6.** Motility parameters of spermatozoa collected from heat-treated mice. Objective sperm motility and velocity was assessed via CASA on spermatozoa from all treatment groups. (A) Motility, (B) progressive motility, (C) average path velocity, (D) straight line velocity, (E) linearity, and (F) amplitude of lateral head displacement. $* P < 0.05$, $** P < 0.01$, $*** P < 0.001$ compared to untreated control.

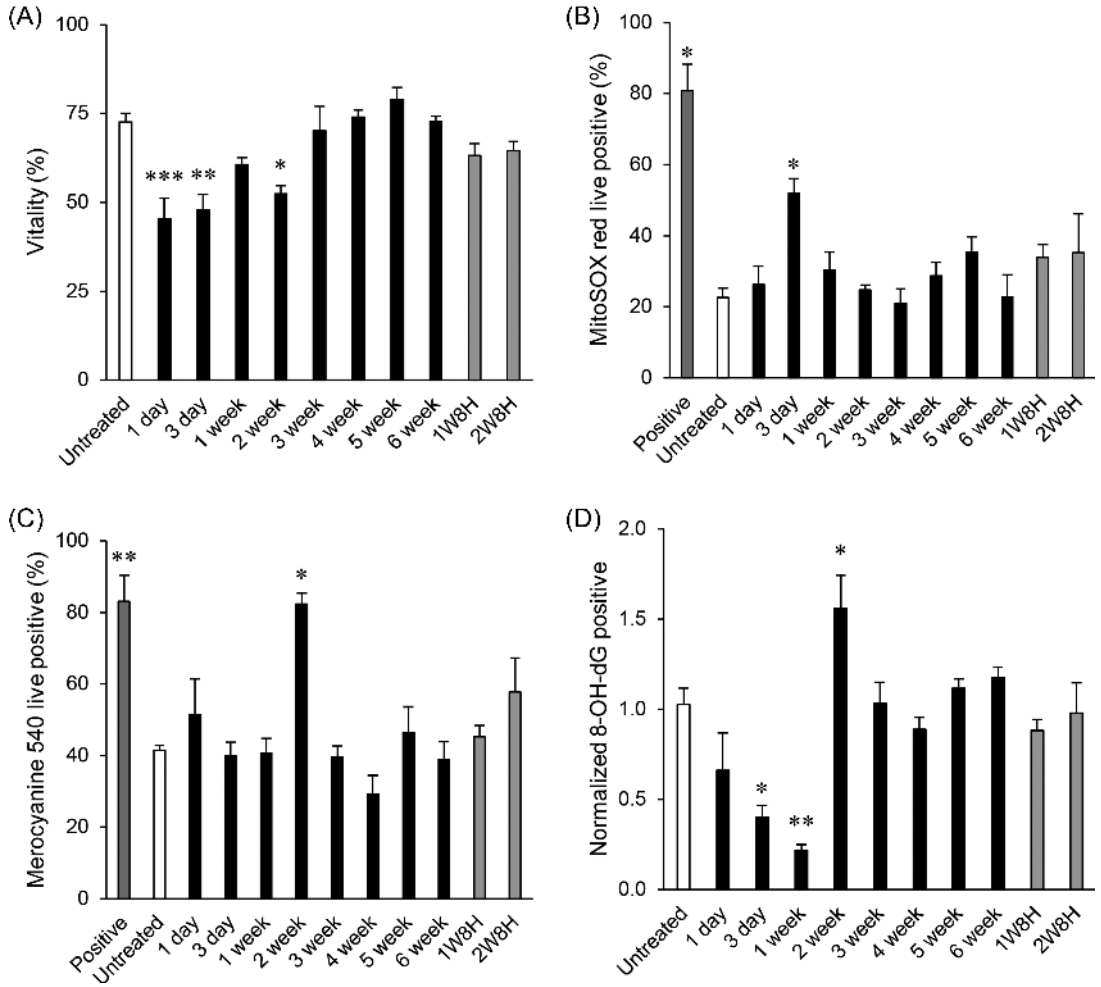


**Figure 7.** The ability of ambient heat treatment to induce oxidative stress in the spermatozoa of mice. (A) Sperm vitality, assessed by the eosin exclusion method. (B) Mitochondrial ROS generation in spermatozoa, detected with the MitoSOX red probe via flow cytometry. (C) Membrane fluidity of spermatozoa, measured with the merocyanine 450 probe via flow cytometry. Arachidonic acid was used as a positive control for panels B and C. (D) Oxidative DNA damage levels, determined by 8-hydroxy-2′-deoxyguanosine antibody labeling to the sperm nuclear DNA (n = 3). The percentage of positive cells was normalized to the untreated control. ∗ $P < 0.05$, ∗∗ $P < 0.01$, ∗∗∗ $P < 0.001$ compared to untreated control.

concert with their highly efficient DNA repair activity in comparison to somatic and late stage germ cells, particularly spermatids [39].

The use of an alternative, chronic heat exposure regimen also led to a loss of sperm motility, irrespective of whether the insult was maintained for 1 or 2 weeks ($P < 0.05$) and is entirely commensurate of the findings of Wechalekar et al. [3, 21]. Furthermore, our complete motility analysis identified a susceptibility to chronic heat exposure over 7–14 days that differed from that documented in acutely exposed mice. During chronic heat exposure, associated heat stress is least damaging when an animal is capable of dissipating thermal energy, generally during the night [40]. When individuals are not capable of undergoing this process, the heat stress propagates as an accumulated heat load and incites cellular stress [41]. This phenomenon is a leading hypothesis to explain chronic thermal cellular stress. Furthermore, our detection of significant reductions to sperm cell quality in both exposure models after 2 weeks firmly implicates the round spermatid population as being a particularly heat-susceptible phase of germ cell development.

The causative relationship between oxidative stress and heat-induced damage of germ cells has previously been established [1, 42], and was further supported by the results reported herein whereby we detected a significant elevation in generation of mitochondrial ROS at 3 days postheating (Figure 7). In accounting for such findings, acute heat stress has been found to induce mitochondrial ROS generation in the liver [43] and skeletal muscle [44] through mechanisms that involve mitochondrial electron transport chain impedance, altered uncoupler protein expression, and elevated activity of electron transport chain complexes 1 and 2 [45]. It is noteworthy that perturbation of both of these complexes is capable of inducing significant electron leakage and associated ROS production [46, 47]. Collectively, these studies reinforce the concept that heat stress alters mitochondrial activity, leading to ROS generation and stimulating a state of oxidative stress.

Our data highlight that spermatozoa sampled 2 weeks after heat stress experience significant reductions in their overall quality. These data add to an emerging body of literature implicating the round spermatid population as being the most susceptible to heat stress [1, 5]. It follows that these cells also display particularly sensitivity to the propagation of oxidative stress due to their abundance of readily oxidized substrates, including an assortment of RNAs and polyunsaturated fatty acids [48], and an open chromatin conformation

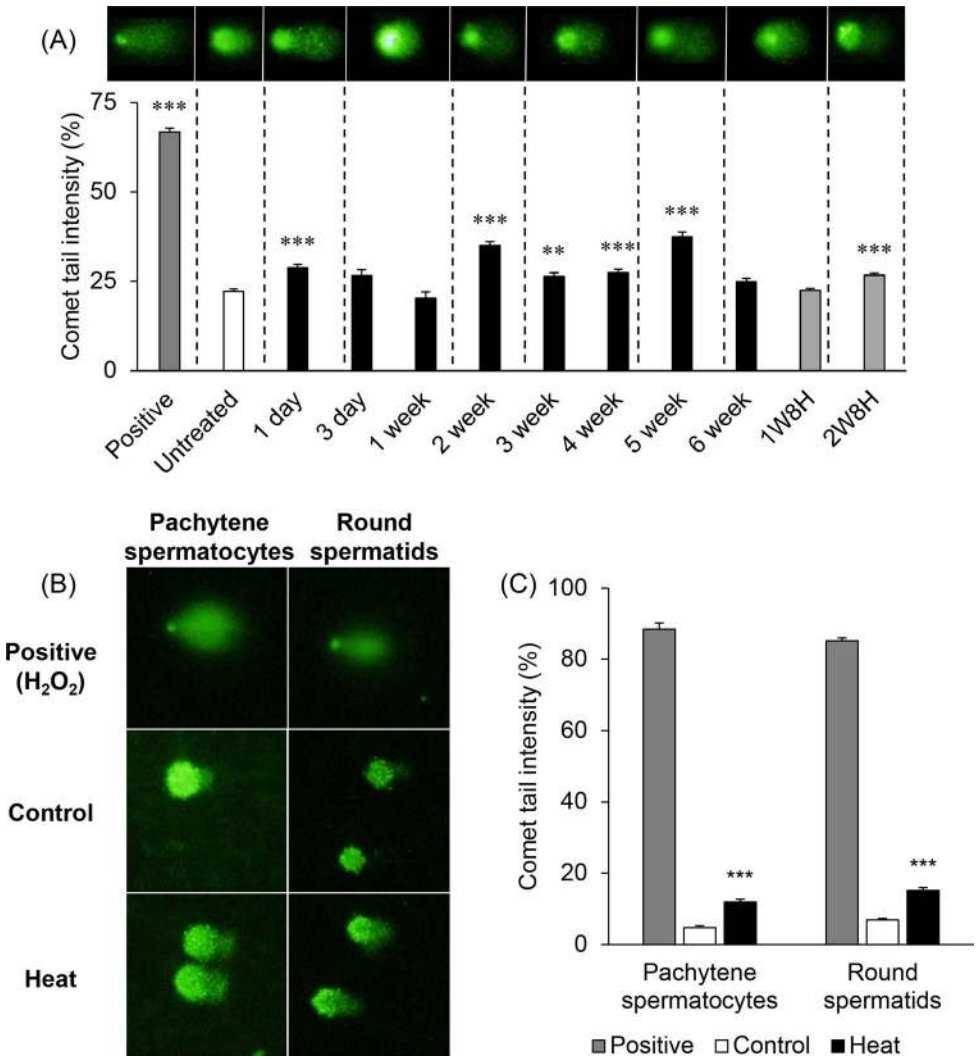


**Figure 8.** DNA fragmentation in heat-treated germ cells and spermatozoa. (A) DNA fragmentation in the form of single-strand breaks was assessed in the spermatozoa of heat-treated mice with the alkaline comet assay. Representative comets are shown above each of the treatments types for both exposure models. Hydrogen peroxide treatment was used as the positive control for this assay. (B) Images of populations of pachytene spermatocytes and round spermatids isolated from 1-day heat recovery testes that were utilized again for the alkaline comet assay. (C) Levels of DNA fragmentation, again in the form of single-strand breaks, were then quantified in these cells (n = 3). $* P < 0.05$, $** P < 0.01$, $*** P < 0.001$ compared to untreated control.

[5]. Compounding this situation, round spermatids also experience declining DNA repair activity as they mature to elongating spermatids [49]. These factors, combined with the subsequent DNA compaction that accompanies elongating spermatid formation [50, 51], place maturing round spermatids in a vulnerable position by allowing these cells to carry damaged DNA throughout their development into spermatozoa [52]. While such lesions have the potential to be transmitted to the zygote via fertilization [53, 54], our study did not reveal any notable reductions in fertilization rates or early embryonic development in an IVF setting. Although these data conflict previous studies [19], it is possible that at the time of fertilization such damage elicited by heat treatment in this study was repaired by the oocyte. Alternatively, the biological significance of this damage may be manifested in the form of mutational load in the subsequent offspring/generation, a possibility that awaits further investigation.

In this study, we have extended the analysis of ambient temperature on reproductive competence by documenting the vulnerability of the male germ line to heat stress and demonstrating that acute heat exposure results in significant modifications to germ cell development, impacting the quality of the spermatozoa produced thereafter. This thermal insult stresses a range of male germ cell types, including spermatogonia, spermatocytes, the terminal spermatozoa, and most notably, the round spermatids. In spermatozoa that were developmentally exposed to heat at the round spermatid stage, significant increases in membrane fluidity and levels of DNA damage were detected. A differential profile was observed with a chronic exposure, which appears to primarily impair multiple aspects of sperm motility and velocity, but also elicits sperm DNA fragmentation after 2 weeks of treatment. As with many studies investigating stresses to spermatogenesis, the damage we uncovered in the spermatozoa was ameliorated when the spermatogonial stem cells matured to gametes. Given that this damage was elicited at temperatures that humans and livestock are routinely exposed to, additional research is required to accurately model real-life conditions and assess the impact of rising ambient temperature on fertility and the developmental normality of the offspring.

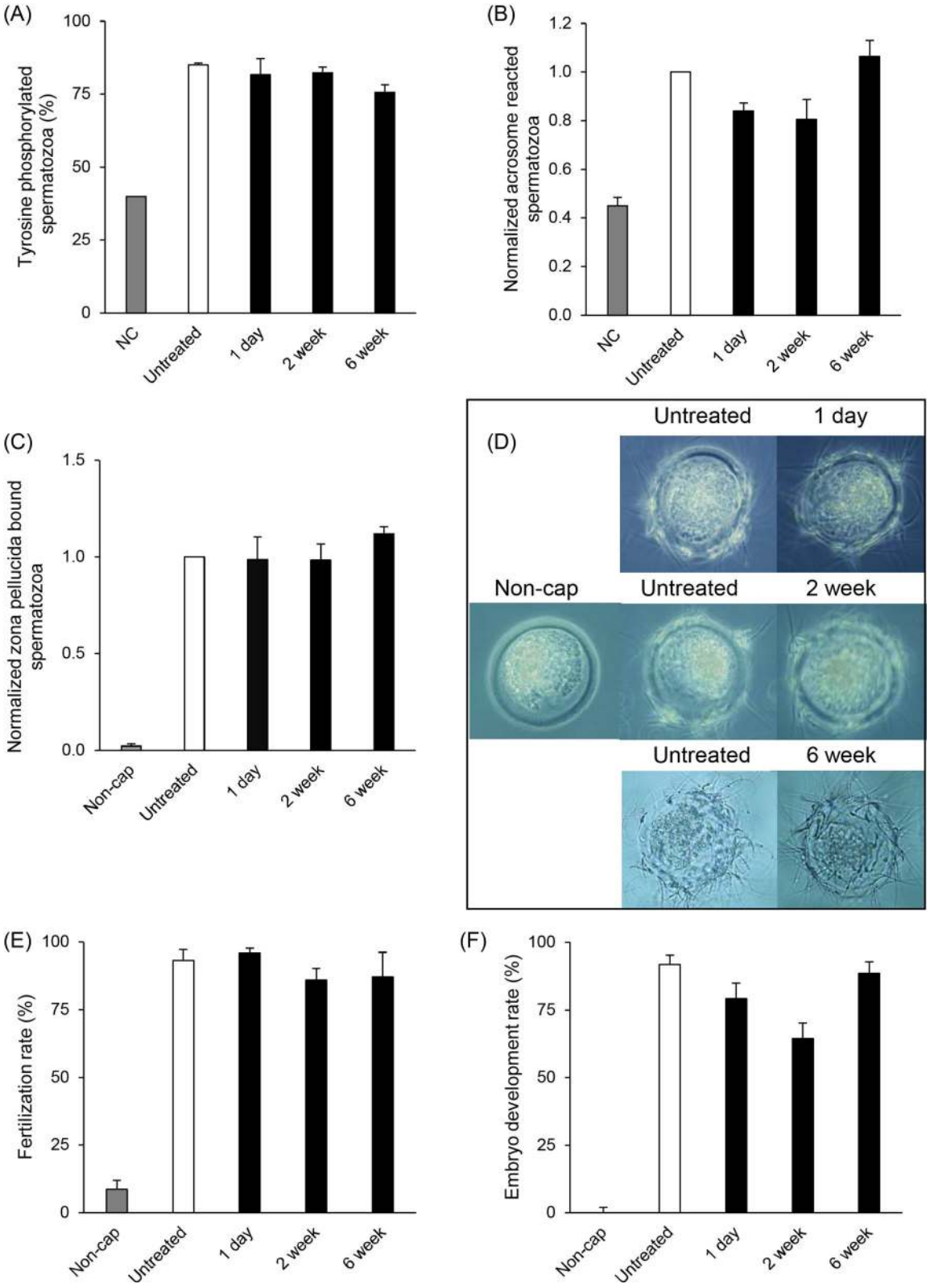


**Figure 9.** The capacitation and fertilization capability of spermatozoa collected from whole body heat-treated mice. Spermatozoa were collected from heat-treated mice at 1 day, 2 weeks, and 6 weeks postinsult and exposed to procapacitation conditions. These groups of spermatozoa were then assessed for their ability to undergo hallmarks of capacitation, achieve binding to the zona pellucida, and, when utilized for IVF, fertilize oocytes and achieve embryonic blastocyst development. (A) Protein tyrosine phosphorylation, a marker of the induction to sperm capacitation. (B) The incidence of the acrosome reaction, normalized to the untreated control. (C) The number of spermatozoa observed bound to the zona pellucida of oocytes, normalized to the untreated control. (D) Representative images of all treatments utilized for the zona binding assay. (E) Oocyte fertilization rate of these spermatozoa when used for IVF. (F) Blastocyst development rate of these zygotes generated via IVF. Each experiment was performed three times (n = 3), except panels E + F 6-week recovery (n = 2).

## Supplementary data

Supplementary data are available at *BIOLRE* online.

**Supplementary Figure S1.** The effect of heat treatment on body temperature. Temperature measurements were taken on mice using an infra-red gun, at the back, armpit, abdomen, and both testes, as well as the external room, and the cage these mice were exposed in. (A) Measurement locations. (B) Temperature readouts prior to (0 h) and during (8 and 24 h) heat treatment.

**Supplementary Figure S2.** The effect of whole body heating on spermatogenesis and testis structure. Mouse testes from 1-day, 2-week, and 6-week heat recovery treatments were fixed and sectioned for staining with a range of stress and structural markers. (A) Hematoxylin and eosin-stained testis sections. (B) Alpha-tubulin testis staining as a structural marker. Scale bar = 200 $\mu$m.

**Supplementary Figure S3.** The effects of whole body heating on epididymal structure. Mouse epididymides from 1-day, 2-week, and 6-week heat recovery treatments were fixed and sectioned for staining to investigate morphological abnormalities using hematoxylin and eosin staining. Images were taken for the three principal regions of this organ: the caput, corpus, and cauda. Scale bar = 100 $\mu$m.

**Supplementary Figure S4.** The effect of whole body heating on testicular cleaved caspase-3 expression. Mouse testes from 1-day, 2-week, and 6-week heat recovery treatments were fixed and sectioned, and then stained for expression of cleaved caspase-3 to detect activation of apoptosis. Scale bar = 200 $\mu$m.

## Acknowledgments

We would like to thank Dr Sally Hall for assistance with the zona binding assay.

**Conflict of Interest:** The authors declare no conflicts of interest that could be perceived as prejudicing the impartiality of the research reported.

## References

1. Hansen PJ. Effects of heat stress on mammalian reproduction. *Philos Trans R Soc B Biol Sci* 2009; **364**:3341–3350.
2. Waites GM. Thermoregulation of the scrotum and testis: studies in animals and significance for man. *Adv Exp Med Biol* 1991; **286**:9–17.
3. Wechalekar H, Setchell BP, Peirce EJ, Ricci M, Leigh C, Breed WG. Whole-body heat exposure induces membrane changes in spermatozoa from the cauda epididymidis of laboratory mice. *Asian J Androl* 2010; **12**:591–598.
4. Gallup GG, Jr, Finn MM, Sammis B. On the origin of descended scrotal testicles: the activation hypothesis. *Evol Psychol* 2009; **7**:517–526.
5. Perez-Crespo M, Pintado B, Gutierrez-Adan A. Scrotal heat stress effects on sperm viability, sperm DNA integrity, and the offspring sex ratio in mice. *Mol Reprod Dev* 2008; **75**:40–47.
6. Zhang MH, Shi ZD, Yu JC, Zhang YP, Wang LG, Qiu Y. Scrotal heat stress causes sperm chromatin damage and cysteinyl aspartate-spicific proteinases 3 changes in fertile men. *J Assist Reprod Genet* 2015; **32**: 747–755.
7. Dada R, Gupta NP, Kucheria K. Spermatogenic arrest in men with testicular hyperthermia. *Teratog Carcinog Mutagen* 2003; **Suppl 1**:235–243.
8. Gyllenborg J, Skakkebaek NE, Nielsen NC, Keiding N, Giwercman A. Secular and seasonal changes in semen quality among young Danish men: a statistical analysis of semen samples from 1927 donor candidates during 1977-1995. *Int J Androl* 1999; **22**:28–36.
9. Jorgensen N, Andersen AG, Eustache F, Irvine DS, Suominen J, Petersen JH, Andersen AN, Auger J, Cawood EH, Horte A, Jensen TK, Jouannet P, Keiding N, Vierula M, Toppari J, Skakkebaek NE. Regional differences in semen quality in Europe. *Hum Reprod* 2001; **16**:1012–1019.
10. Levine RJ, Bordson BL, Mathew RM, Brown MH, Stanley JM, Star TB. Deterioration of semen quality during summer in New Orleans *Fertil Steril* 1988; **49**:900–907.
11. Levine RJ, Mathew RM, Chenault CB, Brown MH, Hurtt ME, Bentley KS, Mohr KL, Working PK. Differences in the quality of semen in outdoor workers during summer and winter. *N Engl J Med* 1990; **323**:12–16.
12. Huang C, Li B, Xu K, Liu D, Hu J, Yang Y, Nie H, Fan L, Zhu W. Decline in semen quality among 30,636 young Chinese men from 2001 to 2015. *Fertil Steril* 2017; **107**:83–88 e82.
13. Virtanen HE, Jorgensen N, Toppari J. Semen quality in the 21st century. *Nat Rev Urol* 2017; **14**:120–130.
14. Walker K. Diagnosis and treatment of sterility in the male. *BMJ* 1928; **2**:652–655.
15. Carmichael CP. Cryptorchidism. *J Natl Med Assoc* 1945; **37**:3–8.
16. Jeffcoate TN. Male Infertility. *BMJ* 1946; **2**:185–191.
17. Setchell BP. The Parkes lecture heat and the testis. *Reproduction* 1998; **114**:179–194.
18. Wettemann RP, Desjardins C. Testicular function in boars exposed to elevated ambient temperature. *Biol Reprod* 1979; **20**:235–241.
19. Zhu B, Walker SK, Oakey H, Setchell BP, Maddocks S. Effect of paternal heat stress on the development in vitro of preimplantation embryos in the mouse. *Andrologia* 2004; **36**:384–394.
20. McLean DJ, Russell LD, Griswold MD. Biological activity and enrichment of spermatogonial stem cells in vitamin a-deficient and hyperthermia-exposed testes from mice based on colonization following germ cell transplantation. *Biol Reprod* 2002; **66**:1374–1379.
21. Wechalekar H, Setchell BP, Pilkington KR, Leigh C, Breed WG, Peirce E. Effects of whole-body heat on male germ cell development and sperm motility in the laboratory mouse. *Reprod Fertil Dev* 2016; **28**:545–555.
22. Smith TB, De Iuliis GN, Lord T, Aitken RJ. The senescence-accelerated mouse prone 8 as a model for oxidative stress and impaired DNA repair in the male germ line. *Reproduction* 2013; **146**:253–262.
23. Biggers JD, Whitten WK, Whittingham DG. The culture of mouse embryos in vitro. In: Daniel JC Jr (ed) *Methods in Mammalian Embryology*. San Francisco: Freeman; 1971: 86–116.
24. World Health Organization. *WHO Laboratory Manual for the Examination and Processing of Human Semen* , 5th edn. Geneva: World Health Organization; 2010: 7–114.
25. Baleato RM, Aitken RJ, Roman SD. Vitamin A regulation of BMP4 expression in the male germ line. *Dev Biol* 2005; **286**:78–90.
26. Katen AL, Chambers CG, Nixon B, Roman SD. Chronic acrylamide exposure in male mice results in elevated DNA damage in the germline and heritable induction of cyp2e1 in the testes. *Biol Reprod* 2016; **95**:86–86.
27. Martin JH, Nixon B, Lord T, Bromfield EG, Aitken RJ. Identification of a key role for permeability glycoprotein in enhancing the cellular defense mechanisms of fertilized oocytes. *Dev Biol* 2016; **417**:63–76.
28. Chirault M, Lucas C, Goubault M, Chevrier C, Bressac C, Lecureuil C. A combined approach to heat stress effect on male fertility in *Nasonia vitripennis*: from the physiological consequences on spermatogenesis to the reproductive adjustment of females mated with stressed males. *PLoS One* 2015; **10**:e0120656
29. Chowdhury AK, Steinberger E. Early changes in the germinal epithelium of rat testes following exposure to heat. *Reproduction* 1970; **22**:205–212.
30. Li W, Wu ZQ, Zhao J, Guo SJ, Li Z, Feng X, Ma L, Zhang JS, Liu XP, Zhang YQ. Transient protection from heat-stress induced apoptotic stimulation by metastasis-associated protein 1 in pachytene spermatocytes. *PLoS One* 2011; **6**:e26013.
31. Li L, Han ZY, Li CM, Jiang XQ, Wang GL. Upregulation of heat shock protein 32 in Sertoli cells alleviates the impairments caused by heat shock-induced apoptosis in mouse testis. *Cell Stress Chaperones* 2013; **18**:333–351.
32. Li Y, Huang Y, Piao Y, Nagaoka K, Watanabe G, Taya K, Li C. Protective effects of nuclear factor erythroid 2-related factor 2 on whole body heat stress-induced oxidative damage in the mouse testis. *Reprod Biol Endocrinol* 2013; **11**:23.
33. Comish PB, Liang LY, Yamauchi Y, Weng CC, Shetty G, Naff KA, Ward MA, Meistrich ML. Increasing testicular temperature by exposure to

elevated ambient temperatures restores spermatogenesis in adult Utp14b (jsd) mutant (jsd) mice. *Andrology* 2015; **3**:376–384.
34. Gao J, Zuo Y, So KH, Yeung WS, Ng EH, Lee KF. Electroacupuncture enhances spermatogenesis in rats after scrotal heat treatment. *Spermatogenesis* 2012; **2**:53–62.
35. Jones R. Sperm survival versus degradation in the mammalian epididymis: a hypothesis. *Biol Reprod* 2004; **71**:1405–1411.
36. Creasy DM. Review article: evaluation of testicular toxicity in safety evaluation studies: the appropriate use of spermatogenic staging. *Toxicol Pathol* 1997; **25**:119–131.
37. Meyerhoeffer DC, Wettemann RP, Coleman SW, Wells ME. Reproductive criteria of beef bulls during and after exposure to increased ambient temperature. *J Anim Sci* 1985; **60**:352–357.
38. Celino FT, Yamaguchi S, Miura C, Ohta T, Tozawa Y, Iwai T, Miura T. Tolerance of spermatogonia to oxidative stress is due to high levels of Zn and Cu/Zn superoxide dismutase. *PLoS One* 2011; **6**: e16938.
39. Rube CE, Zhang S, Miebach N, Fricke A, Rube C. Protecting the heritable genome: DNA damage response mechanisms in spermatogonial stem cells. *DNA Repair* 2011; **10**:159–168.
40. Gaughan JB, Mader TL, Holt SM, Lisle A. A new heat load index for feedlot cattle. *J Anim Sci* 2008; **86**:226–234
41. Hahn GL, Mader TL. Heat waves in relation to thermoregulation, feeding behavior and mortality of feedlot cattle. In: Bottcher RW, Hoff SJ (eds.), *Livestock Environment V. Proceedings of the 5th International Symposium*. Bloomington, MN: American Society of Agricultural Engineers; 1997: 563–571.
42. Paul C, Teng S, Saunders PT. A single, mild, transient scrotal heat stress causes hypoxia and oxidative stress in mouse testes, which induces germ cell death. *Biol Reprod* 2009; **80**:913–919.
43. Yang L, Tan GY, Fu YQ, Feng JH, Zhang MH. Effects of acute heat stress and subsequent stress removal on function of hepatic mitochondrial respiration, ROS production and lipid peroxidation in broiler chickens. *Comp Biochem Physiol C Toxicol Pharmacol* 2010; **151**: 204–208.
44. Mujahid A, Akiba Y, Toyomizu M. Olive oil-supplemented diet alleviates acute heat stress-induced mitochondrial ROS production in chicken skeletal muscle. *Am J Physiol Regul Integr Comp Physiol* 2009; **297**:R690–R698.
45. Hawkins TD, Warner ME. Warm preconditioning protects against acute heat-induced respiratory dysfunction and delays bleaching in a symbiotic sea anemone. *J Exp Biol* 2017; **220**:969–983.
46. Quinlan CL, Perevoshchikova IV, Hey-Mogensen M, Orr AL, Brand MD. Sites of reactive oxygen species generation by mitochondria oxidizing different substrates. *Redox Biol* 2013; **1**:304–312.
47. Quinlan CL, Goncalves RLS, Hey-Mogensen M, Yadava N, Bunik VI, Brand MD. The 2-oxoacid dehydrogenase complexes in mitochondria can produce superoxide/hydrogen peroxide at much higher rates than Complex I. *J Biol Chem* 2014; **12**:8312–8325.
48. Nixon B, Bromfield EG, Dun MD, Redgrove KA, McLaughlin EA, Aitken RJ. The role of the molecular chaperone heat shock protein A2 (HSPA2) in regulating human sperm-egg recognition. *Asian J Androl* 2015; **17**:568–573.
49. Marchetti F, Bishop J, Gingerich J, Wyrobek AJ. Meiotic interstrand DNA damage escapes paternal repair and causes chromosomal aberrations in the zygote by maternal misrepair. *Sci Rep* 2015; **5**:7689.
50. Aitken RJ, Curry BJ. Redox regulation of human sperm function: from the physiological control of sperm capacitation to the etiology of infertility and DNA damage in the germ line. *Antioxid Redox Signal* 2011; **14**:367–381.
51. Zini A, Libman J. Sperm DNA damage: clinical significance in the era of assisted reproduction. *CMAJ* 2006; **175**:495–500.
52. Leduc F, Nkoma GB, Boissonneault G. Spermiogenesis and DNA repair: a possible etiology of human infertility and genetic disorders. *Syst Biol Reprod Med* 2008; **54**:3–10.
53. Aitken RJ, De Iuliis GN, McLachlan RI. Biological and clinical significance of DNA damage in the male germ line. *Int J Androl* 2009; **32**:46–56.
54. Lord T, Aitken RJ. Fertilization stimulates 8-hydroxy-2′-deoxyguanosine repair and antioxidant activity to prevent mutagenesis in the embryo. *Dev Biol* 2015; **406**:1–13.